WHITE PAPER

Cryo-EM sample optimization using the VitroEase Buffer Screening Kit

by Atieh Amininan, Dimple Karia, Xue Wang, Albert Konijnenberg, Natalya Dudkina
Editor: Alex Ilitchev

Introduction

Sample preparation is currently a major bottleneck in cryo-electron microscopy (cryo-EM) single particle analysis (SPA). Even purified proteins that are stable and structurally intact can behave differently in a thin vitreous ice layer, exhibiting unwanted behavior such as denaturation, aggregation, or preferred orientation.[1,2] Due to the unique properties of each protein, multiple rounds of optimization are often necessary, where vitrification parameters, grid types, or additives are adjusted before the optimal condition for high-resolution data collection are found (*i.e.* particles are structurally intact, randomly oriented and equally distributed). Currently, sample optimization is often performed in a non-systematic way, extending optimization time over multiple days or even weeks.[2] To reduce this, we have developed a detergent and buffer screening kit for a broad range of pH and ionic strengths. The Thermo Scientific™ VitroEase™ Buffer Screening Kit was designed to optimize screening, by utilizing the instrument's Autoloader systems and Thermo Scientific EPU Multigrid Software (*PN 1264046*), in order to minimize microscope time.

Current cryo-EM samples optimization techniques

Various experimental approaches are currently used to overcome the challenges of cryo-EM sample preparation. One common technique changes the type of holey cryo-EM grid used while adjusting hole size and support film material.[3] The addition of a thin layer of carbon, hydrophilized graphene, or graphene oxide, for instance, can alter protein adsorption to the support film and prevent protein denaturation during vitrification; it can also protect the protein from the air-water interface.[3-6] Besides varying the sample carrier, multiple rounds of sample application are also used, but require further optimization of vitrification conditions.[7]

In many cases, vitrification is optimized by adjusting the temperature and humidity during sample preparation, and/or changing the blotting time and force used in the Thermo Scientific Vitrobot™ System. Further optimization can also be done at the protein level; for instance, cross-linking reagents can be added prior to vitrification to stabilize fragile macromolecules.[8] For small proteins with a molecular weight <100 kDa, antibodies can be appended to increase sample mass.[9] With so many different parameters for optimization, it can be difficult to quickly arrive at optimal condition.

Design of a buffer optimization kit for cryo-EM samples

Previous studies have shown that different buffer conditions (*e.g.* changing pH or salt concentration) can impact protein stability by changing the surface charge of the protein and thereby altering its behavior in ice.[10-13] Here, we present a systematic approach for optimizing cryo-EM samples for SPA. We offer preselected, ready-to-use buffers and detergents (Tables 1 and 2) which decrease the number of optimization iterations needed during cryo-EM sample preparation of water-soluble proteins. The included buffers span a broad range of pH and ionic strengths and have been selected based on a large-scale literature study, which included over 800 cryo-EM papers published from 2014 to 2019 (data not shown). These premade buffers can be used to systematically identify optimal protein vitrification conditions. The VitroEase Buffer Screening Kit offers a screening strategy that has been designed for EPU Multigrid Software, which enables unattended EM image acquisition for 12 grids within one working day. EPU Multigrid Software is available on Thermo Scientific microscopes equipped with Autoloader systems, including the Thermo Scientific Krios™, Glacios™, and Talos Arctica™ Cryo-TEMs.

Note: It is recommended that protein homogeneity and stability are verified with other techniques such as negative stain EM or native mass spectrometry prior to vitrification, in order to increase sample optimization efficiency.[14] Furthermore, the final optimized conditions will vary based on sample type; in order to obtain a high-resolution structure, optimization will need to be carried out for each type of sample individually.

ThermoFisher SCIENTIFIC

Table 1. Buffers for cryo-EM sample optimization

Buffer 1	Buffer 2	Buffer 3	Buffer 4
50 mM sodium acetate 150 mM NaCl pH 3.6	50 mM sodium acetate 300 mM KCl pH 3.6	50 mM MES 150 mM NaCl pH 5.5	50 mM MES 300 mM NaCl pH 5.5
Buffer 5	**Buffer 6**	**Buffer 7**	**Buffer 8**
50 mM Tris-HCL 10 mM Mg(CH3COO)2 150 mM NaCl pH 7.2	50 mM Tris-HCl 10 mM MgCl2 150 mM CH3CO2K pH 7.2	50 mM Tris-HCL 10 mM Mg(CH3COO)2 300 mM KCl pH 7.2	50 mM HEPES 150 mM NaCl pH 7.4
Buffer 9	**Buffer 10**	**Buffer 11**	**Buffer 12**
50 mM HEPES 300 mM KCl pH 7.4	50 mM HEPES 5 mM Mg(CH3COO)2 150 mM CH3CO2K pH 7.4	50 mM HEPES 5 mM MgCl2 5 mM CaCl2 150 mM NaCl pH 7.4	4.3 mM Na2HPO4 137 mM NaCl 2.7 mM KCl pH 7.4
Buffer 13	**Buffer 14**		
50 mM Bicine 150 mM NaCl pH 8.5	50 mM CAPSO 300 mM KCl pH 8.9		

Table 2. Detergents for cryo-EM sample optimization

Detergents	Class/head group	CMC
CTAB (Hexadecyltrimethylammonium bromide)	Cationic	0.03%
CHAPS ((3-[(3-cholamidopropyl)dimethylammonio]-1-propanesulfonate))	Zwitterionic	0.49%
β-OG (octyl β-D-glucopyranoside)	Non-ionic	0.27%
Tween 20 (polyoxyethylene 20)	Non-ionic	0.01%
DM (n-decyl-ß-D-maltoside)	Non-ionic	0.09%
FOM (fluorinated octyl maltoside)	Non-ionic	0.07%

Table 3. Recommended screening strategy

	First screening round (recommended conditions*)		Second screening round (suggested detergent conditions)
1	Protein with lower concentration (1 mg/mL) in the purification buffer	**1**	Buffer* + 0.5× CMC of CTAB
2	Protein with higher concentration (≤10 mg/mL) in the purification buffer	**2**	Buffer* + 0.75× CMC of CTAB
3	Buffer 1 or Buffer 2, pH 3.6	**3**	Buffer* + 0.5× CMC of CHAPS
4	Buffer 3 or Buffer 4, pH 5.5	**4**	Buffer* + 0.75× CMC of CHAPS
5	Buffer 6, pH 7.2	**5**	Buffer* + 0.25× CMC of FOM
6	Buffer 7, pH 7.2	**6**	Buffer* + 0.5× CMC of FOM
7	Buffer 10 or Buffer 11, pH 7.4	**7**	Buffer* + 0.25× CMC of Tween 20
8	Buffer 13, pH 8.5	**8**	Buffer* + 0.5× CMC of Tween 20
9	Buffer 14, pH 8.9	**9**	Buffer* + 0.25× CMC of β-OG
10	Buffer 5, pH 7.2 + 0.1× CMC of β-OG or + 0.75× CMC of DM	**10**	Buffer* + 0.75× CMC of β-OG
11	Buffer 8, pH 7.4 + 0.75× CMC of Tween 20 or + 0.75× CMC of FOM	**11**	Buffer* + 0.25× CMC of DM
12	Buffer 9, pH 7.4 + 0.1× CMC of CHAPS or + 0.1× CMC of CTAB	**12**	Buffer* + 0.5× CMC of DM

**Best conditions determined during the first screening round*

Table 4. Selection of compounds incompatible with cryo-EM

Compounds	Acceptable Concentration
Glycerol	Below 2%
Salt	Below 500 mM
Glucose	Below 5%
Sucrose	Below 5%

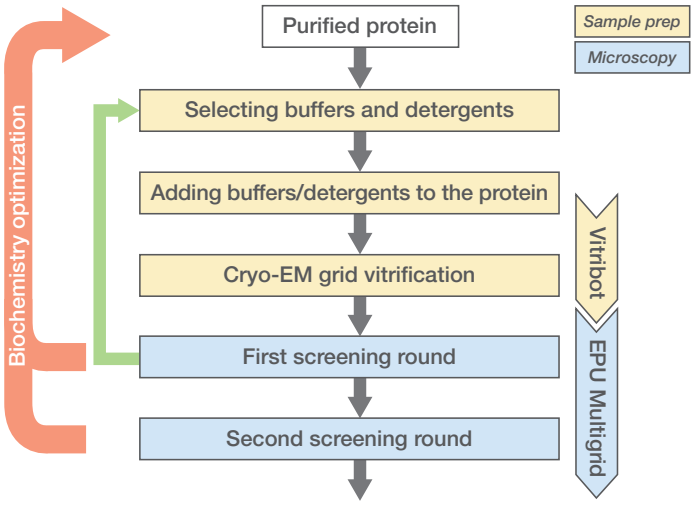

Figure 1. Workflow of sample optimization with the VitroEase Buffer Screening Kit.

Cryo-EM sample optimization protocol using the VitroEase Buffer Screening Kit: Suggested screening strategy

The workflow overview in Figure 1 depicts the individual steps required for cryo-EM sample optimization using the VitroEase Kit. To follow the screening strategy shown in Table 3, the user begins by selecting several buffer and three detergents from Tables 1 and 2. These are then added to the protein solution prior to vitrification. For the second screening round, the user selects one buffer (based on the outcome of the first screening round) and then combines it with six detergents at different concentrations. In many cases, this structured approach can reduce screening to 24 grids (spread over two Autoloader cassettes) over the course of 24 hours. (When performed automatically with EPU Multigrid Software.) The outcome of the screening either provides the user with a cryo-EM grid that can be used for data acquisition or redirects the user to upstream optimization of the sample.

First screening round

1. Optimizing protein concentration

Protein concentration is an important parameter that needs to be optimized in the early stages of a cryo-EM project. Generally, it is worth increasing protein concentration, as it has been shown that high concentrations can improve protein stability and distribution on the cryo-EM grid.[15] Begin by preparing a grid at typical cryo-EM protein concentrations (*i.e.* between 0.5-2 mg/mL); this should provide a good particle distribution and will serve as a reference point for all further optimization. The second grid should be prepared at the highest available protein concentration (*i.e.* up to 10 mg/mL). These two conditions can be used to determine if the protein is amenable to close packing (sometimes referred to as a carpet or monolayer), a state that has been shown to support thin ice and, subsequently, high-resolution data collection.

The observed number of particles on the grid often differs from the expected density (based on the protein concentration in the bulk solution) due to the hydrophobicity of the grid surface, the affinity of the protein for the EM grid support, and absorbance of the protein to the blotting paper. The impact of these can vary depending on vitrification settings such as blotting time and force.[16,17] While the expected number of particles found in the grid holes can be estimated for a given sample concentration and size, this has to be verified by screening on the microscope.[17]

When preparing cryo-EM samples, it is important to remove compounds that can reduce image contrast. Table 4 shows a selection of compounds that can have adverse effects on vitrification and/or subsequent imaging (*i.e.* glycerol, sugars, or buffers with very high ionic strength).[3,17,18] These compounds can be removed using buffer exchange columns, dialysis cassettes, or molecular weight cutoff spin columns before the buffers are used.

2. Increasing protein integrity in ice

The VitroEase Kit contains buffers with a pH range between 3.6 and 8.9, pre-mixed with various salts and divalent cations. As it is still not fully understood how buffer conditions impact vitrification, buffer optimization will need to be done for each type of protein (independent of upstream protein-purification optimization) to ensure the structural and biochemical integrity of the protein in vitreous ice.[19]

The proposed screening strategy, as shown in Table 3, tests 10 different pre-mixed buffers in order to obtain optimal protein distribution and to verify protein integrity in vitreous ice. Although this approach uses a broad range of preselected conditions, it still requires the user to make some decisions. The user should choose at least one buffer that closely resembles the purification buffer and then select 6 pH values that are combined with lower (150 mM) or higher (300 mM) salt concentrations.

> **Example screening:**
> Begin by selection a buffer with a low pH (*e.g.* Buffer 3 with 50 mM MES, 150 mM NaCl and pH 5.5). Then, select a buffer with the same pH but with a different salt concentration to test the impact of ionic strength on proteins stability (*e.g.* Buffer 4 with 50 mM MES, 300 mM KCl, and pH 5.5). Subsequently, several buffers with a neutral pH should be tested to see the protein's behavior with the addition of cationic ions.

The buffer that gave the best results in the first round of screening can be used for detergent screening in the second round. If no improvement is observed in the first screening round, it is recommended that sample stability and integrity are optimized in the upstream protein purification step. Alternatively, different detergents can be chosen in the second screening round, or different optimization approaches can be attempted, such as the addition of a thin carbon, hydrophilized graphene, or graphene oxide layer, which can alter protein behavior in vitreous ice.

We tested the 20S proteasome of *Thermoplasma acidophilum* in order to illustrate the effect that buffers can have on protein behavior in vitreous ice. The protein was vitrified on Quantifoil R1.2/1.3 Grids (SPT Labtech, UK) with the Thermo Scientific Vitrobot Mk IV System at a protein concentration of 1 mg/mL. To exclude the impact of ice thickness on protein behavior, grid areas with a similar ice thickness were selected based on their gray values. When vitrified in its purification buffer, the sample contained significant quantities of the intact 20S proteasome dimer, as is shown in Figure 2A. Although usable, these dimers make it more difficult to reconstruct the protein. The use of various buffers showed that adjusting pH and ionic strength altered the behavior of the protein in vitreous ice (Figure 2).

The impact of unsuitable buffers on the 20S proteasome ranged from protein aggregation, to poor particle distribution, to induced preferred orientation in ice. Figure 2E demonstrates that a high pH buffer led to visible aggregation of T20S, whereas intact and homogenous particles were observed in a more suitable buffer (Figure 2C). These particles were stable, had random orientation, and were equally separated, making them suitable for high resolution data acquisition.

3. Detergent screening to prevent particle interaction with the air-water interface

A common approach for adjusting protein orientation in vitreous ice is the addition of detergents below critical micelle concentrations (CMC).[20,21]

Detergents improve the quality of the prepared cryo-EM grids through two mechanisms. First, they reduce collision with the air-water interface, which can otherwise lead to partial denaturation of the protein.[3,20,22] Second, they increase grid surface hydrophilicity.[21,23] These mechanisms can also influence particle orientation, reducing a sample's preferred orientation and thereby improving the 3D reconstruction.

Six commonly used detergents are included as part of the VitroEase Kit (Table 2). In the first screening round (Table 3), three detergents should be used to evaluate their impact on protein behavior and to accelerate decision making during the second screening round. Detergents can be selected based on their charge and concentration. In particular, detergents with a low and high CMC, at two different concentrations, should be evaluated. For example, one grid can be vitrified with either octyl-β-glucopyranoside (a detergent with a high CMC value) at 0.1× CMC or n-Decyl-β-D-Maltoside (a detergent with a low CMC value) at 0.75× CMC concentration. The second grid could be vitrified with one non-ionic detergent (*e.g.* Tween-20 or FOM at 0.75× CMC). The third grid could then be vitrified with a cationic or zwitterionic detergent (e.g. CTAB or CHAPS at 0.1 x CMC).

Having a detergent in the vitrification buffer may decrease the number of particles in vitreous ice.[21] Using detergents in the first screening round can guide detergent and protein concentrations in the second round. If the number of particles decrease after a detergent is added, the protein concentration could be increased. Similarly, if the addition of detergents did not improve particle orientation in the first screening round, detergent concentrations can be increased up to their CMC values in the second screening round. If there was visible improvement, then the first screening result will dictate buffer and detergent selection for the second round.

Note: Changing solution pH and/or adding detergents can impact the structure and function of the sample protein. It is recommended that, once optimal conditions for cryo-EM are found, a biochemical assay is used to verify that protein function has been maintained.

Second screening round

In the second screening round, different detergents should be used in combination with the optimized buffer identified in the first round (*i.e.* the buffer that resulted in the best protein behavior in ice, with equal particle distribution, random orientation, and no visible protein aggregation or disintegration). All six detergents should be used at two concentrations in the second screening round; in this way, detergent concentration can be optimized based on the outcome of the first screening round.

We used the SARS-CoV-2 spike protein to show the impact that detergents can have on protein behavior. The protein was vitrified on UltraAuFoil R0.6/1 Grids (SPT Labtech, UK)

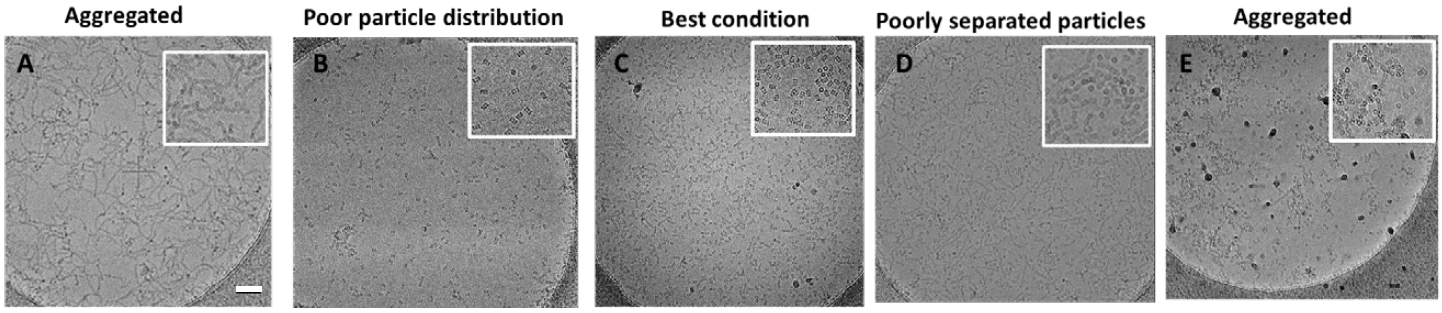

Figure 2. Cryo-EM micrographs of the *Thermoplasma acidophilum* T20S proteasome in various buffers as part of the first screening round. (**A**) T20S in 50 mM Tris-acetate buffer, 150 mM NaCl, 5 mM DTT at pH 6.8. (**B**) T20S in Buffer 5 (50 mM Tris-HCL, 10 mM Mg(CH3COO)2, 150 mM NaCl at pH 7.2) with 1 mM of added DTT. (**C**) T20S in Buffer 10 (50 mM HEPES, 5 mM Mg(CH3COO)2, 150 mM CH3CO2K at pH 7.4) with 1 mM added DTT. (**D**) T20S in Buffer 11 (50 mM HEPES, 150mM NaCl, 10 mM Mg(CH3COO)2 at pH 7.4) with 1 mM added DTT. (**E**) T20S in Buffer 14 (50 mM CAPSO, 300 mM KCl at pH 8.9) with 1 mM added DTT. Scale bar represents 100 nm.

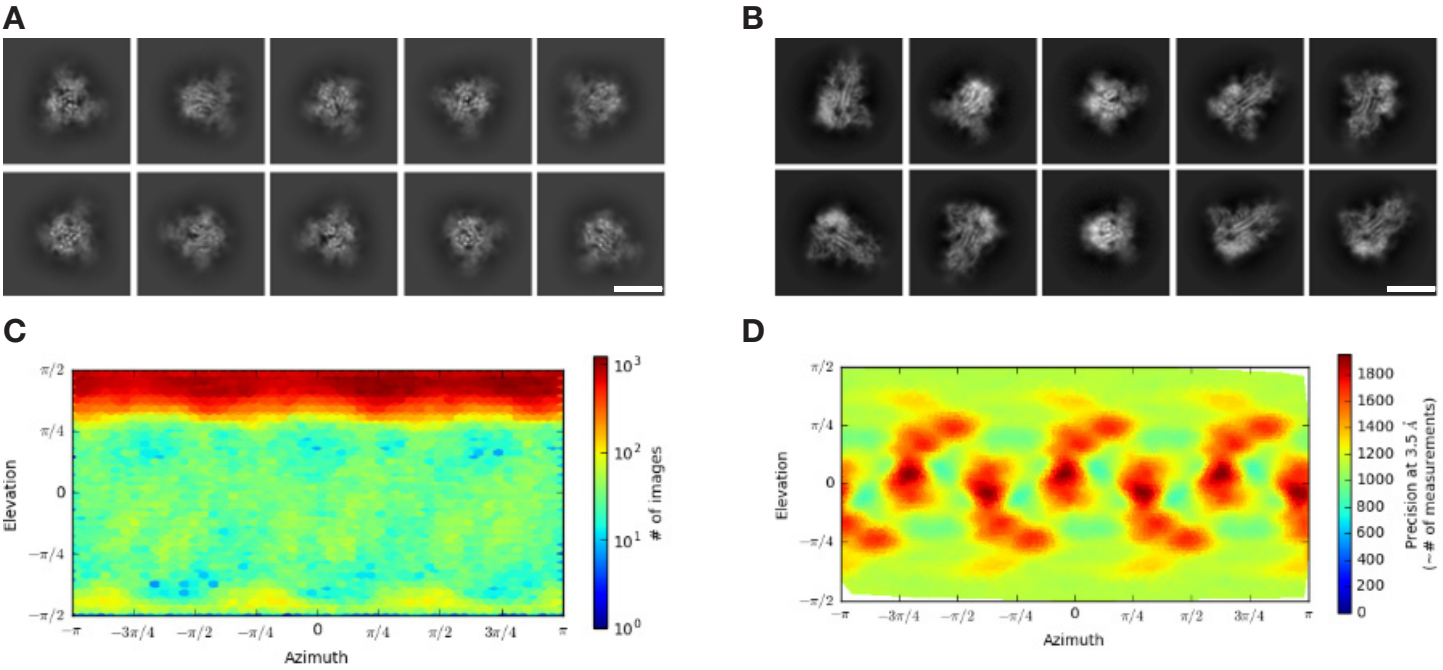

Figure 3. Cryo-EM analysis of SARS-CoV-2 spike protein. (**A**) 2D classes before sample optimization. (**B**) 2D classes after the addition of CHAPS (1× CMC). (**C**) Distribution of angles before sample optimization. (**D**) Distribution of angles after sample optimization. Scale bar represents 10 nm.

with the Vitrobot Mk IV System at a concentration of 7 mg/mL. Initial sample evaluation revealed that the majority of particles were in the same orientation, which would hinder a high-resolution 3D reconstruction (Figure 3A,C). To adjust this, various VitroEase detergents were tested. The angular distribution (Figure 3C) was improved by the addition of CHAPS at 1× CMC and a high-resolution 3D reconstruction could be produced. These results demonstrate that structured screening of detergents can help optimize the cryo-EM sample.

Using various buffers and detergents for fatty acid synthase

To further demonstrate the VitroEase workflow, a fatty acid synthase (FAS) sample from *Saccharomyces cerevisiae* was prepared for cryo-EM imaging. Previous research by Dr. Martin Grininger of Goethe University (Frankfurt, Germany) showed that FAS adsorbs to the air-water interface during vitrification, resulting in partial protein denaturation and preferential orientation in ice.[22] They were able to overcome these issues through combined optimization of protein expression and purification, as well as the use of graphene coated grids. Our experiments sought to determine if similar results can be obtained using the VitroEase Kit.

First, 1.7 mg/mL FAS was vitrified on Quantifoil R0.6/1 Grids (SPT Labtech, UK) using the Vitrobot Mk IV System with buffer conditions determined in the first screening round (Table 3). Identical ice thickness was selected by visual assessment of the grid squares in order to avoid any impact of variable thickness on protein behavior. The cryo-EM images (Figure 4A) and 2D classification (Figure 6A) of the protein showed that the particles are structurally intact and equally distributed in ice, but only side views are visible. The first screening round showed that changing buffer type, pH, and salt did not impact particle orientation (Figure 4B-D). Particle distribution did change with particle number, however, decreasing in Buffer 14 (Figure 4D) and increasing in Buffer 7 and 11 (Figure 4B,C).

The most promising protein distribution was found in Buffer 9 (50 mM HEPES and 300 mM KCl at pH 7.4), which was subsequently selected for the second screening round. Three detergents were tested in the first screening round: 0.75× CMC Tween 20, 0.1× CMC CHAPS (Figure 4E,F), and 0.75× CMC DM. Addition of 0.75× CMC DM and 0.75× CMC Tween 20 (Figure 4E) decreased the number of particles with no improvement in particle orientation. Using this information, detergent concentration were decreased for the second screening round to 0.5× CMC (Figure 5B,C).

Figure 5 demonstrates the effect that different detergents had at similar CMC while maintain the same protein concentration, buffer, and grid type. The non-ionic detergent FOM (Figure 5A) and cationic CTAB (Figure 5D) did not change the number of particles in ice when used at similar CMC. The non-ionic detergent Tween 20 (Figure 5C), meanwhile, visibly reduced the number of particles on the grid at the same CMC value.

These results once again highlight the difficulty of predicting how different detergents will impact protein behavior in ice, and the need for screening. To verify the effect of cryo-EM sample optimization, a small data set was collected in a buffer containing 50 mM HEPES and 300 mM KCl at pH 7.4

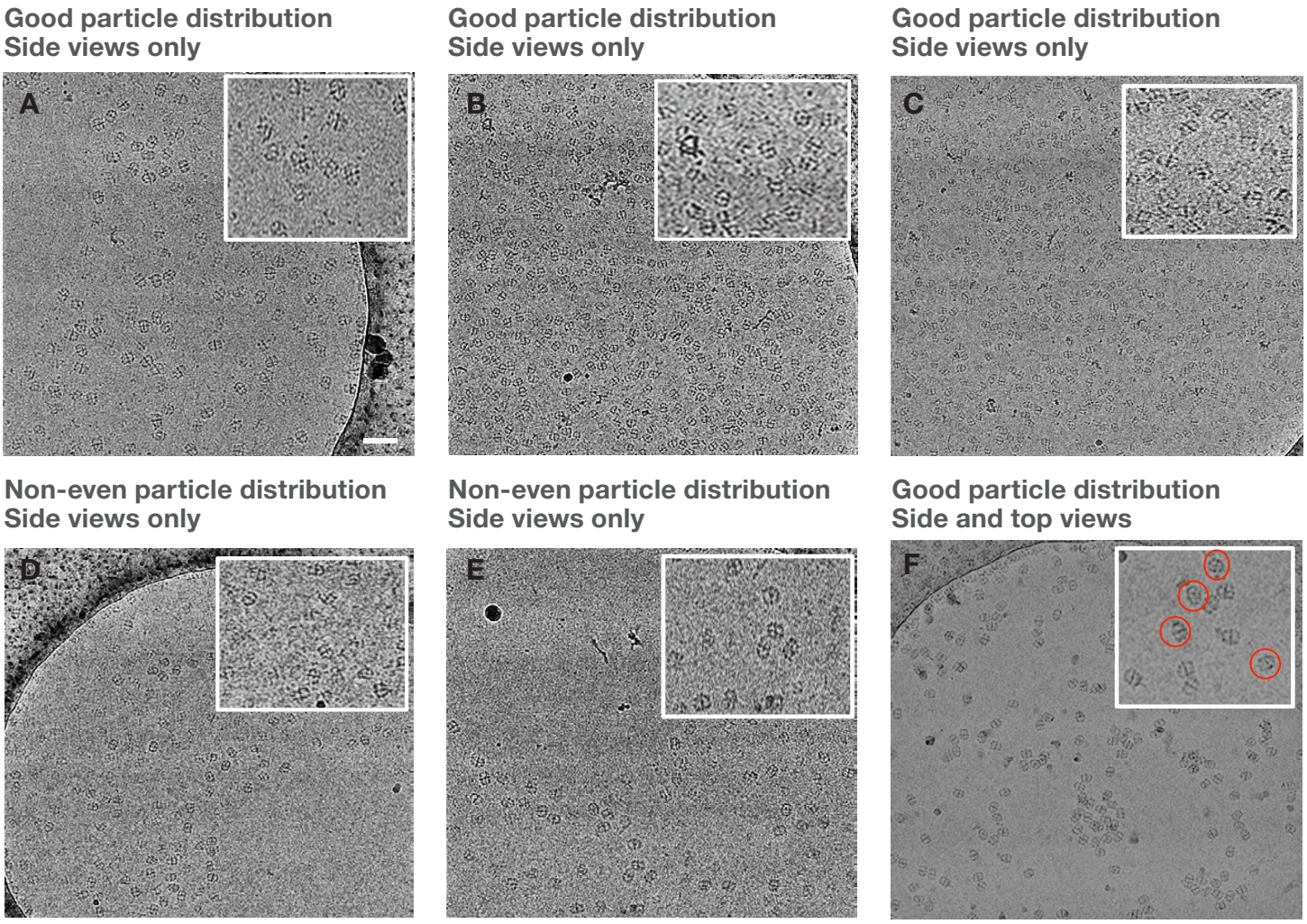

Figure 4. Cryo-EM micrographs of fatty acid synthase in different buffers. (**A**) FAS in purification buffer (50 mM sodium phosphate at pH 6.5). (**B**) FAS in Buffer 11 (50 mM HEPES, 5 mM MgCl2, 5 mM CaCl2, pH 7.4). (**C**) FAS in Buffer 7 (50mM Tris-HCl, 10 mM Mg(CH3COO)2, 300 mM KCl at pH 7.2). (**D**) FAS in Buffer 14 (50mM CAPSO, 300 mM KCl at pH 8.9). (**E**) FAS in Buffer 9 (50 mM HEPES, 300 mM KCl at pH 7.4) with 0.75× CMC Tween 20. (**F**) FAS in Buffer 9 (50 mM HEPES, 300 mM KCl at pH 7.4) with 0.1× CMC CHAPS. Red circles indicate side, top and tilted particle views. Scale bar represents 100 nm.

with 0.5× CMC CHAPS. The data was processed using Relion 3.1 Software.24 The 2D classes obtained from 41,071 particles showed different particle orientations with top and side views (Figure 6B). In comparison, the control dataset before optimization only showed side views (Figure 6A). By following the recommended screening protocol, the sample was optimized within two days of screening and could be used for high-resolution data collection.

Finally, to verify the effect of different grid types, 1.7 mg/mL FAS protein was vitrified on UltrAuFoil R0.6/1 Grids (SPT Labtech, UK) with the Vitrobot Mk IV System, using the same vitrification settings as the general screening strategy. No change of particle orientation was observed using the same buffer with different grid types.

Conclusion

Sample preparation for single particle cryo-EM is a major bottleneck, as there are many variables which can negatively influence the collection of high-quality data. Without a systematic approach, the process of optimization can be time consuming, expensive, and has a low probability of successfully identifying optimal conditions. The VitroEase Buffer Screening Kit provides a structured protocol for the identification of buffer and additive conditions for cryo-EM sample preparation, which is critical for successful structural determination. When used in conjunction with EPU Multigrid Software, the time spent on sample optimization can be reduced to as little as 24 hours and doesn't require direct user interaction. In future, the combination of vitrification automation, Autoloader systems, smarter EPU MultiGrid Software, and a fully automated processing pipelines will enable even more EM samples to be optimized within a shorter time frame.

Acknowledgements

We thank Dr. Martin Grininger (Goethe University Frankfurt, Germany) for providing us with fatty acid synthase and Prof. Kuang Shen (University of Massachusetts Medical School, USA) for the SARS-CoV-2 spike protein used in this work.

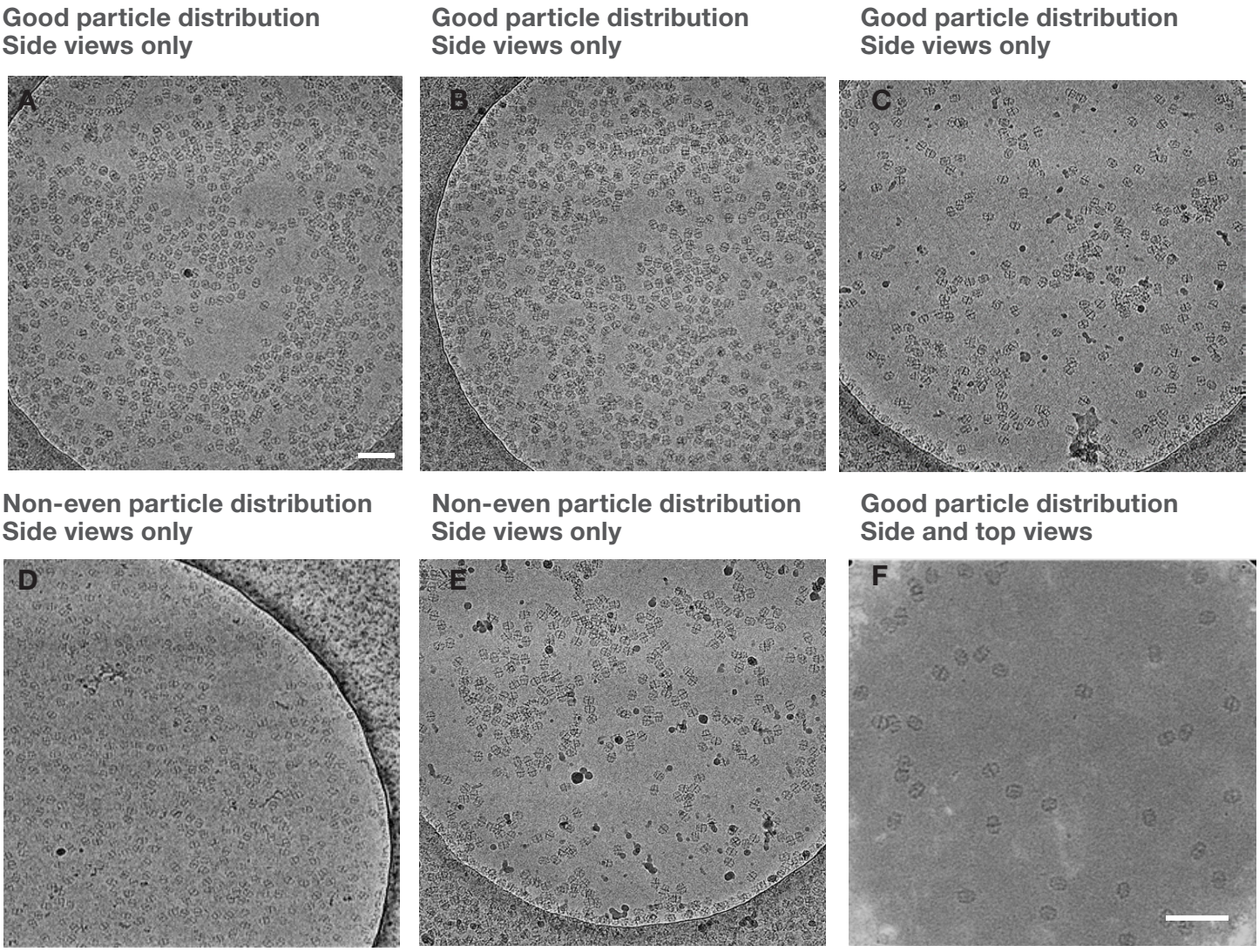

Figure 5. Cryo-EM micrographs of fatty acid synthase in Buffer 9 and various detergents as part of the second screening round. Protein concentration is 1.7 mg/mL in all panels. (**A**) Detergent = 0.5× CMC FOM. (**B**) Detergent = 0.5× CMC DM. (**C**) Detergent = 0.5× CMC Tween 20. (**D**) Detergent = 0.5× CMC CTAB. (**E**) Detergent = 0.5× CMC β-OG (**F**) Detergent = 0.5× CMC CHAPS. Scale bar represents 100 nm in panels A and F.

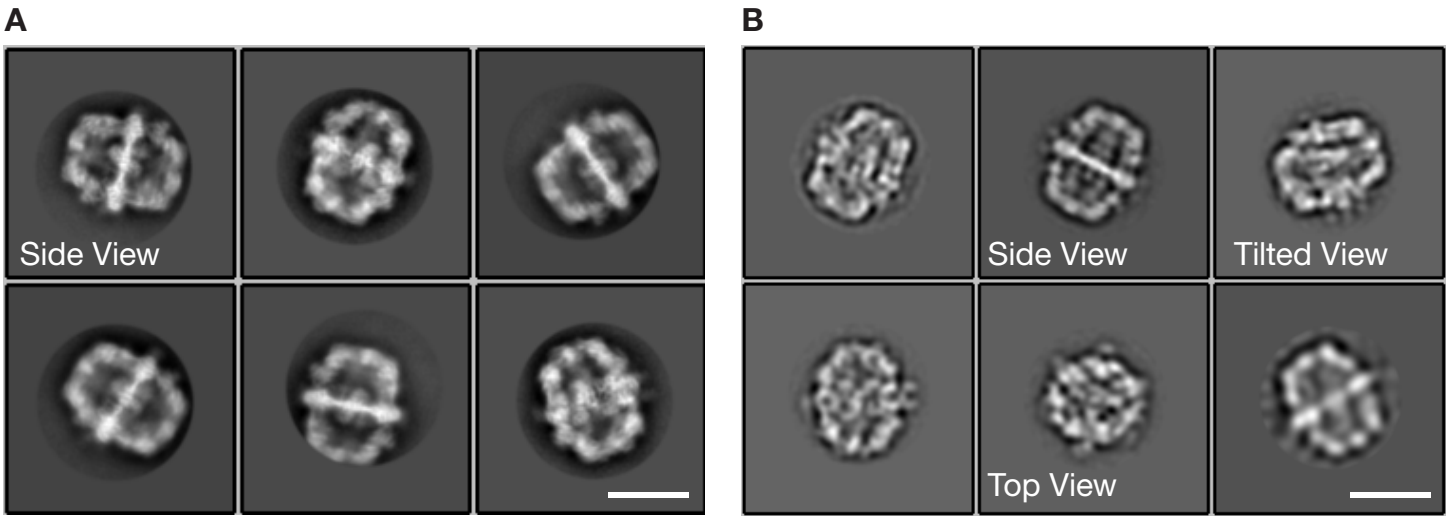

Figure 6. Cryo-EM analysis of fatty acid synthase. 1.7 mg/mL FAS was vitrified on UltrAuFoil R0.6/1 Grids with the Vitrobot Mk IV System. (**A**) 2D classes in purification buffer (50 mM sodium phosphate at pH 6.5) before sample optimization. (**B**) 2D classes after sample optimization with Buffer 9 (50 mM HEPES, 300 mM KCl at pH 7.4) with 0.5× CMC CHAPS. Scale bar represents 20 nm.

thermo scientific

References

1. B. Carragher et al., "Current outcomes when optimizing 'standard' Cryo-EM specimen preparation for single-particle cryo-EM.," J. Microsc., vol. 276, no. 1, pp. 39–45, Oct. 2019, doi: 10.1111/jmi.12834.
2. S. A. Arnold et al., "Miniaturizing EM Cryo-EM specimen Preparation: Opportunities, Challenges, and 'Visual Proteomics'.," Proteomics, vol. 18, no. 5–6, p. e1700176, Mar. 2018, doi: 10.1002/pmic.201700176.
3. Drulyte et al., "Approaches to altering particle distributions in cryo-electron microscopy Cryo-EM specimen preparation," Acta Crystallogr. Sect. D, Struct. Biol., vol. 74, no. Pt 6, pp. 560–571, Jun. 2018, doi: 10.1107/S2059798318006496.
4. E. Palovcak et al., "A simple and robust procedure for preparing graphene-oxide cryo-EM grids," J. Struct. Biol., vol. 204, no. 1, pp. 80–84, 2018, doi: https://doi.org/10.1016/j.jsb.2018.07.007.
5. R. Pantelic, J. Meyer, U. Kaiser, W. Baumeister, and J. Plitzko, "Graphene oxide: A substrate for optimizing preparations of frozen-hydrated Cryo-EM specimen s," J. Struct. Biol., vol. 170, pp. 152–156, Apr. 2010, doi: 10.1016/j.jsb.2009.12.020.
6. C. J. Russo and L. A. Passmore, "Controlling protein adsorption on graphene for cryo-EM using low-energy hydrogen plasmas," Nat. Methods, vol. 11, no. 6, pp. 649–652, 2014, doi: 10.1038/nmeth.2931.
7. J. Snijder et al., "Vitrification after multiple rounds of Cryo-EM specimen application and blotting improves particle density on cryo-electron microscopy grids.," J. Struct. Biol., vol. 198, no. 1, pp. 38–42, Apr. 2017, doi: 10.1016/j.jsb.2017.02.008.
8. H. Stark, "GraFix: stabilization of fragile macromolecular complexes for single particle cryo-EM.," Methods Enzymol., vol. 481, pp. 109–126, 2010, doi: 10.1016/S0076-6879(10)81005-5.
9. S. Wu et al., "Fabs Enable Single Particle cryoEM Studies of Small Proteins," Structure, vol. 20, no. 4, pp. 582–592, 2012, doi: 10.1016/j.str.2012.02.017.
10. Teddy J. Zbacnik, Charles S. Henry, Mark Cornell Manning, "Role of Buffers in Protein Formulations," Journal of Pharmaceutical Sciences, Volume 106, Issue 3,2017, Pages 713-733. doi: 10.1016/j.xphs.2016.11.014
11. Deller MC, Kong L, Rupp B. "Protein stability: a crystallographer's perspective," Acta Crystallogr F Struct Biol Commun. 2016;72(Pt 2):72-95. doi:10.1107/S2053230X15024619
12. Stina Lindman, Wei-Feng Xue, Olga Szczepankiewicz, Mikael C. Bauer, Hanna Nilsson, Sara Linse, "Salting the Charged Surface: pH and Salt Dependence of Protein G B1 Stability," Biophysical Journal,2006, Pages 2911-2921. doi.org/10.1529/biophysj.105.071050
13. Passmore LA, Russo C, "Specimen Preparation for High-Resolution Cryo-EM," Methods Enzymol. 2016; 579():51-86. doi: 10.1016/bs.mie.2016.04.011
14. https://assets.thermofisher.com/TFS-Assets/CMD/Application-Notes/an-65947-lc-ms-mnesi-native-protein-complexes-an65947-en.pdf
15. L.Y. Kim et al. "Benchmarking cryo-EM single particle analysis workflow," Front.Mol.Biosci vol.5, pp 1-8, Jun 2018, https://doi.org/10.3389/fmolb.2018.00050
16. D. P. Klebl et al., "Need for Speed: Examining Protein Behavior during CryoEM Grid Preparation at Different Timescales," Structure, vol. 28, no. 11, pp. 1238-1248.e4, 2020, doi: 10.1016/j.str.2020.07.018.
17. K. R. Vinothkumar and R. Henderson, "Single particle electron cryomicroscopy: trends, issues and future perspective.," Q. Rev. Biophys., vol. 49, p. e13, Jan. 2016, doi: 10.1017/S0033583516000068.
18. R. A. Grassucci, D. J. Taylor, and J. Frank, "Preparation of macromolecular complexes for cryo-electron microscopy.," Nat. Protoc., vol. 2, no. 12, pp. 3239–3246, 2007, doi: 10.1038/nprot.2007.452.
19. V. Martins de Oliveira, V. de Godoi Contessoto, F. Bruno da Silva, D. L. Zago Caetano, S. Jurado de Carvalho, and V. B. Pereira Leite, "Effects of pH and Salt Concentration on Stability of a Protein G Variant Using Coarse-Grained Models," Biophys. J., vol. 114, no. 1, pp. 65–75, 2018, doi: 10.1016/j.bpj.2017.11.012.
20. R. M. Glaeser, "Proteins, interfaces, and cryo-em grids," Curr. Opin. Colloid Interface Sci., vol. 34, pp. 1–8, Mar. 2018, doi: 10.1016/j.cocis.2017.12.009.
21. M. Cheung et al., "A method to achieve homogeneous dispersion of large transmembrane complexes within the holes of carbon films for electron cryomicroscopy," J. Struct. Biol., vol. 182, no. 1, pp. 51–56, Apr. 2013, doi: 10.1016/j.jsb.2013.01.004.
22. E. D'Imprima, D. Floris, M. Joppe, R. Sánchez, M. Grininger, and W. Kühlbrandt, "The deadly touch: protein denaturation at the water-air interface and how to prevent it," bioRxiv, 2018, doi: 10.1101/400432.
23. M. Joppe et al., "The resolution revolution in cryoEM requires high-quality Cryo-EM specimen preparation: a rapid pipeline to a high-resolution map of yeast fatty acid synthase," IUCrJ, vol. 7, no. Pt 2, pp. 220–227, Mar. 2020, doi: 10.1107/S2052252519017366.
24. J. Zivanov, T. Nakane, B. Forsberg, D. Kimanius, W.J.H. Hagen, E. Lindahl & S.H.W. Scheres (2018) "RELION-3: new tools for automated high-resolution cryo-EM structure determination," eLife 7:e42166. doi: 10.7554/eLife.42166.001
25. J. R. Castón, "Conventional electron microscopy, cryo-electron microscopy and cryo-electron tomography of viruses," Subcell. Biochem., vol. 68, pp. 79–115, 2013, doi: 10.1007/978-94-007-6552-8_3.
26. R. M. Glaeser and B.-G. Han, "Opinion: hazards faced by macro-molecules when confined to thin aqueous films," Biophys. Reports, vol. 3, no. 1, pp. 1–7, 2017, doi: 10.1007/s41048-016-0026-3.

Find out more at **thermofisher.com/EM-sales**

ThermoFisher SCIENTIFIC